American Mineralogist, Volume 59, pages 1242–1248, 1974

Zoned Lithium-Aluminum Mica Crystals from the Pala Pegmatite District

KENNETH J. BROCK

Department of Geology, Indiana University Northwest, Gary, Indiana 46408

Abstract

Mica crystals from the Tourmaline Queen mine have monocrystalline muscovite cores surrounded by pinkish rims of intergrown lepidolite crystallites. The central muscovite has the $2M_1$ structure and is bounded by well formed {110} and {010} faces on which lepidolite has developed through epitaxial overgrowth. Lepidolite rims usually consist of $1M + 2M$ mixtures, but one sample contained only the $1M$ structure and had $a = 5.227 \pm 0.002$ Å, $b = 9.020 \pm 0.003$ Å, $c = 10.118 \pm 0.002$ Å, and $\beta = 100° 46' \pm 1'$; muscovite parameters from this crystal were $a = 5.182 \pm 0.004$ Å, $b = 8.997 \pm 0.004$ Å, $c = 20.073 \pm 0.007$ Å, and $\beta = 95° 45' \pm 2'$. Lepidolite crystallites are twinned about ⟨310⟩ and are attached to muscovite (110) on a plane in the zone $\langle 1\bar{1}0 \rangle$, possibly (110).

The lepidolite rims contain significantly more Mn, Rb, and polylithionite than the central muscovite; although outer portions of the muscovite core are slightly enriched in polylithionite, the major compositional change occurs abruptly at the interface between micas. Closely associated zoned tourmaline, consisting of schorl cores surrounded by alkali tourmaline, suggests that the zoned micas were formed by crystallization from two fluids of different composition; however, polylithionite enrichment in the outermost muscovite implies that the transition between fluids may have been gradual.

Introduction

Visibly zoned lithium-bearing mica crystals, consisting of muscovite cores encased in pink lepidolite, were described from Haddam Neck, Connecticut, by Bowman (1902), and similar crystals have been reported by Jahns and Wright (1951, p. 34) from the Pala district in southern California. In each occurrence the zoned crystals appeared in or near pockets within complex pegmatites associated with zoned tourmaline. Lepidolite typically contains 4.0 to 7.7 percent Li_2O and is comprised of the $1M$, $2M_2$, or $3T$ polymorphs, whereas muscovite possesses the $2M_1$ structure and normally contains less than 3.3 percent Li_2O, suggesting that the zoning reflects both compositional and structural changes within the mica.

The presence of zoned lithium-aluminum micas indicates variable conditions during crystallization from the parent pegmatitic fluid and raises the possibility that a detailed investigation of the zoning might yield information regarding the formation of complex pegmatites. This paper reports results of a crystal chemical investigation of zoned lithium-aluminum mica crystals from the Pala district and discusses geologic implications of the zoning.

Occurrence

Samples studied in this investigation were collected from the dump of the Tourmaline Queen mine (located on Queen Mountain *ca* 3 km north of Pala), and were not observed in place; however, Jahns and Wright (1951, p. 57) report the occurrence of similarly zoned crystals in pocket-bearing portions (in and immediately beneath the core) of this pegmatite.

Typical crystals occur in lavender colored books averaging about 20 mm in maximum dimension; cleaved books reveal that the lavender color is restricted to the outer 1 or 2 mm of the crystal and that the (001) cleavage plane is continuous across both rim and core. Cleavage flakes often exhibit diamond-shaped outlines due to well developed {110} faces on the muscovite; {010} faces are also occasionally present truncating acute angles between {110} faces (Fig. 1). Except for the absence of an external surface composed of fibrous rose-colored muscovite, these crystals are remarkably similar to those described by Bowman (1902).

Associated minerals include compact aggregates of lepidolite flakes, massive quartz, prismatic tourmaline crystals, and albite. The albite generally appears

as platy cleavelandite crystals less than 10 mm across, but fine-grained sugary masses of this feldspar were detected in several samples. Colored mica rims invariably appear only along the margins of mica crystals in direct contact with cleavelandite and are absent when the crystal abuts against quartz. A single hand sample may contain pink, green, and black tourmaline prisms, and occasionally conspicuously zoned crystals revealing black schorl cores surrounded by thin successive zones of green and pink alkali-tourmaline are observed.

Color Zoning

Microscopic examination indicates that boundaries between the central muscovite and the lilac-colored rim consist of distinct planes parallel to the {110} and {010} muscovite forms (see Fig. 1). Each muscovite core is composed of a single crystal which exhibits uniform extinction, whereas rims are comprised of a mosaic of small (usually <1 mm across) irregularly shaped crystallites, which rarely attain complete extinction and often display highly distorted interference figures. Crystallites near the rim-muscovite boundary are generally smaller and yield more highly distorted interference figures than those occurring farther from the boundary. Distorted interference figures and the failure to extinguish suggest that most crystallites consist of intergrown mica flakes of different crystallographic orientation (Bloss, Gibbs, and Cummings, 1963). Optic angles vary between 37 and 50° for the crystallites and were consistently near 45° in the muscovite.

X-ray powder data from the colored rims of four separate mica crystals indicate the presence of either a $1M$ polymorph or a mixture of $1M$ and $2M$ micas.[1] Two samples contained $1M + 2M_1$ mixtures and may have also contained the $2M_2$ polymorph which cannot be detected in a $2M_1 + 2M_2$ mixture using powder data. A third sample consisted of a $1M + 2M_2$ mixture, and the remaining sample (P-05) contained only the $1M$ polymorph. In all cases powder data from the muscovite cores were consistent with the $2M_1$ structure. Powder patterns of the $1M$ mica are similar to the synthetic trilithionite pattern tabulated by Munoz (1968, p. 1498); unit cell parameters for sample P-05 are listed in Table 1.

[1] Distinction between polymorphs was based on the presence or absence of key strong reflections as outlined by Munoz (1968, p. 1947).

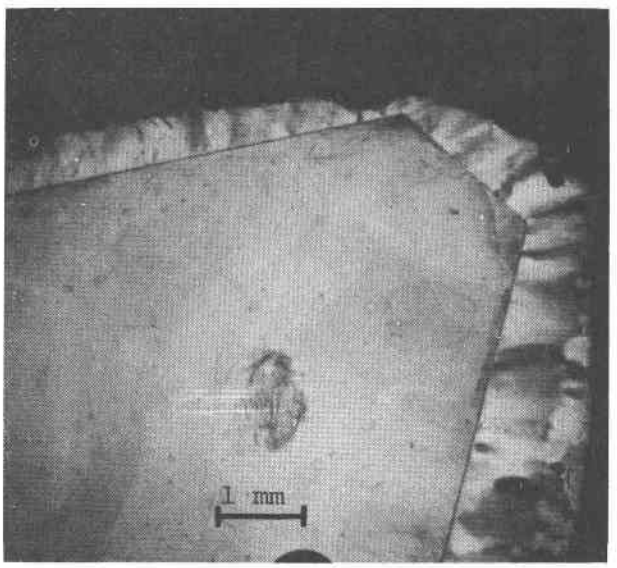

FIG. 1. Photomicrograph of zoned Li-mica crystal revealing a central muscovite core bounded by {110} and {010} faces surrounded by an external rim composed of lepidolite crystallites. Note the absence of irregularities and embayments on the muscovite faces. The blemish near the center of the muscovite is an abrasion on the cleavage surface.

Chemical Variations Within Mica Crystals

Crystal P-05 was selected for chemical study because it contained a single lepidolite polymorph ($1M$) and also exhibited a particularly deep violet outer rim. Electron microprobe traverses along path **a-a'** in Figure 2 were conducted in order to detect qualitative changes in Si, Al, Mn, K, and Rb across the crystal. Approximate SiO_2, Al_2O_3 and MnO concentrations along the traverse were estimated by

TABLE 1. Chemical and Physical Properties of Crystal P-05

	$2M_1$ Muscovite Core	1M Lepidolite Rim
Atomic absorption analysis (wt. %)		
SiO_2	43.7	47.3
Al_2O_3	34.9	22.8
MnO	.48	3.34
Li_2O	.26	4.76
Cell dimensions		
a	5.182±0.004 Å	5.227±0.002
b	8.997±0.004 Å	9.020±0.003
c	20.073±0.007 Å	10.118±0.002
β	95°45±2'	100°46±1'
V	931.2±.2 Å^3	468.7±.2 Å^3

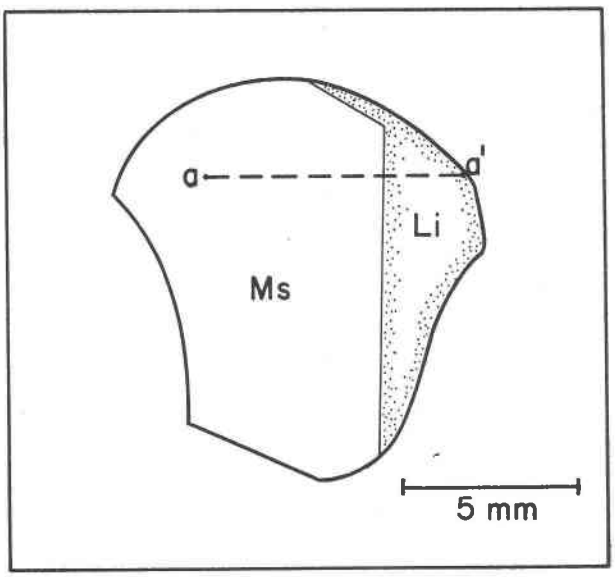

FIG. 2. Sketch showing electron microprobe analytical traverse **a-a'** across sample P-05.

comparing the microprobe data with atomic absorption analyses performed on samples cut from an adjacent cleavage flake (see Table 1). K:Rb ratios were approximated by comparing microprobe intensities with an analyzed muscovite. The microprobe data are not quantitative; consequently, interpretation must be based on chemical variations across the crystal rather than on absolute values. The analytical profile along the traverse was checked by monitoring Al on two additional scans parallel to **a-a'**; in each case the results were essentially identical, indicating that variations in analytical values along the traverse are reproducible.

Si, Al, and Li Variations

Figure 3 reveals an abrupt drop in Al concentration at the muscovite-lepidolite interface. The traverse also shows a gradual decrease in Al content of the muscovite directly adjacent to the mica boundary suggesting that the outermost muscovite is enriched in lithium; however, the absence of Li analyses limits direct substantiation of this contention. Lithium variations across the mica crystal can be evaluated indirectly providing Si and Al analyses and transformed into Li-mica conponents. Foster (1960), Munoz (1968), and Rieder (1970) report that the composition of lithium aluminum micas can be accurately expressed by three components: polylithionite (Pl) $K_2Li_4Al_2Si_8O_{20}(OH,F)_4$, trilithionite (Tl) $K_2Li_3Al_3Si_6Al_2O_{20}(OH,F)_4$, and muscovite (Ms) $K_2Al_4Si_6Al_2O_{20}(OH)_4$.

Examination of Li-mica analyses from the literature reveals a high correlation between Al:Si atomic ratio and mole percent Pl in natural lithium micas.[2] 55 Li-mica analyses, each containing less than 1.25 percent Fe_2O_3 + FeO and analysis summations between 99.0 and 101.0 percent, were selected from the literature, and mole percent Pl was regressed on Al:Si atomic ratio (R), yielding the following least squares quadratic equation

$$Pl = 153.005 - 245.233(R) + 93.241(R)^2 \pm 2.3 \quad (1)$$

Variations in Pl content across sample P-05, calculated from Eq. (1) using Si and Al data from microprobe analyses, are shown in Figure 3 and indicate a gradual increase in Pl content as the mica boundary is approached. This suggests that the outer 1 mm of the muscovite core is in fact enriched in lithium relative to central portions of the crystal. The major increase in Pl content, however, occurs abruptly at the muscovite-lepidolite boundary indicating a substantial increase in Li content at the interface between phases.

The high correlation between Pl content and Al:Si atomic ratio in natural Li-micas can be attributed to the fact that lines of equal Al:Si ratio are nearly parallel to the Tl-Ms join on a triangular Pl-Tl-Ms diagram (*i.e.*, Tl and Ms have similar Al:Si ratios) and that natural micas containing more than 50 mole percent Tl are rare. Rieder (1970, p. 140) reaches a similar conclusion based on crystal chemical arguments and eliminates Tl entirely, plotting the Pl-Tl-Ms triangle on a single Pl-Ms join.

K, Rb, and Mn Variations

Within the limits of experimental error, variation in K:Rb ratio was not detected across either mica, but the Rb concentration was low and subtle variations may have been undetected. Figure 3 does reveal, however, that the K:Rb ratio in the lepidolite rim is about 50 percent below K:Rb values observed in the muscovite core. Potassium content was essentially constant throughout the traverse; consequently, the abrupt decrease in K:Rb ratio observed at the mica interface is due entirely to higher Rb concentration within the lepidolite rim.

[2] Pl content was determined from the relation Pl = 50 (Si-6), where Si represents the number of Si cations per mica formula. The cation content of each analysis was calculated assuming $24O^{-2}$, $2K^+$, and $4H^+$ ions per formula.

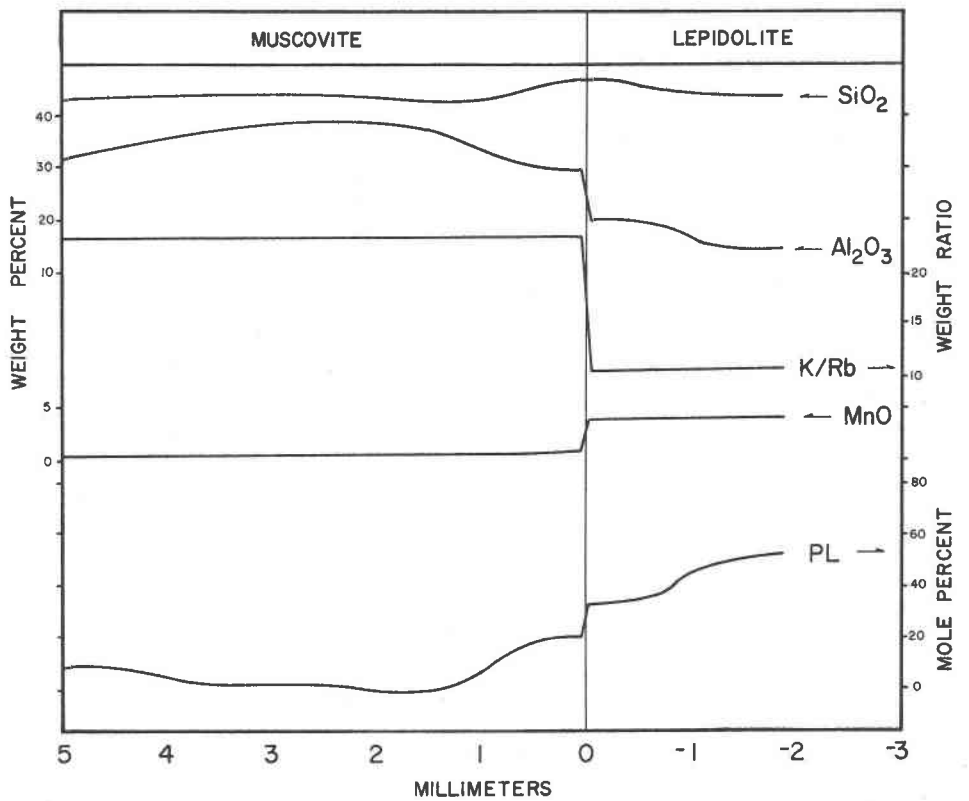

FIG. 3. Schematic presentation of compositional changes calculated from electron microprobe traverse along path a-a' shown in Fig. 2. Origin of the millimeter scale is the muscovite-lepidolite interface. PL represents polylithionite component.

Rb enrichment in the outer rim may be in part attributed to the availability of larger interlayer cation sites, which more easily accommodate Rb ion in the lepidolite structure. Crystal structure analyses of micas have revealed a general correlation between the tetrahedral rotation angle (α) and a decrease in size of the interlayer cation site. The tetrahedral rotation angle of muscovite is near 13° (Radoslovich, 1960), whereas Takeda, Haga, and Sadanaga (1971) report α rotation angles of 3 and 5.3° respectively for the $1M$ and $2M_2$ lepidolite structures. $1M$ micas generally exhibit smaller α-angles than muscovite (McCauley and Newnham, 1971) and, therefore, possess larger interlayer cation sites. Partitioning of the large Rb ion between biotite (typically a $1M$ structure) and muscovite was clearly demonstrated by Gresens and Stensrud (1971) who reported Rb contents of 260 and 640 ppm respectively for intergrown muscovite-biotite portions of a single mica crystal from the Mitchell Creek pegmatite, Georgia.

Muscovite within 1 mm of the lepidolite boundary shows a very slight increase in Mn; however, the major change in Mn content occurs abruptly at the mica interface. The relatively high Mn content in lepidolite rims undoubtedly accounts for their pink or lavender color (sample P-05 possessed a particularly deep violet rim). Correlation between the typical lavender, pink, or lilac lepidolite colors and Mn content was made by Heinrich and Levinson (1953) and has subsequently been confirmed by Faye (1968) through comparison of the optical absorption spectra of lepidolite and $Mn(OH_2)_6^{2+}$. Although rose-colored $2M_1$ muscovite has been reported, it is relatively uncommon, suggesting that lepidolite possesses a greater capacity for incorporating Mn into octahedral sites than does the $2M_1$ structure.

Hazen and Wones (1972) point out that cations with radii greater than 0.78 Å are too large for the octahedral sites in trioctahedral micas; they also note an inverse relation between α and R^{2+} radii in stable trioctahedral micas. If the correlation between α and R^{2+} can be extrapolated to the dioctahedral micas,

then the octahedral sites in lepidolite (transitional between dioctahedral and trioctahedral) must be somewhat larger than the corresponding 6-fold sites in muscovite. This suggests that the characteristic pink colors typically associated with lepidolite may reflect a preferential accommodation of Mn ion owing to the availability of larger octahedral sites.

Orientation of Crystallites

The planar nature of the inter-mica boundary seems to indicate that the lepidolite fringes were formed by simple epitaxial[3] overgrowth rather than through topotactic reaction between parent muscovite and late pegmatitic solutions. It is difficult to conceive of topotactic lepidolite development without the introduction of irregularities and embayments in the faces of the host muscovite crystals.

Many crystallites within the lepidolite rim are not in direct contact with the muscovite core; however, in all cases the optic planes of crystallites yielding undistorted interference figures are related by a rotation of approximately 60° about $\perp$ (001). According to Deer, Howie, and Zussman (1962) the optic axial plane in lepidolite is parallel to (010); Černy, Rieder, and Povondra (1970, p. 324) also report that monoclinic micas violating O.A.P. parallel to (010) are not observed along the siderophyllite-polylithionite join. Based on the assumption that O.A.P. is parallel to (010) in the lepidolite rims, ⟨100⟩ directions were determined in several crystallites within the rims of seven different mica flakes using an optical technique similar to the method employed by Bloss *et al* (1963). Without exception ⟨100⟩ directions between crystallites were related by 120°, indicating the crystallites are twinned about a ⟨310⟩ axis (mica twin law).

The most extensively developed muscovite form is {110}; consequently, the majority of lepidolite crystallites which attach directly to muscovite must join (110) muscovite faces. Microscopic observations indicate the optic planes of the crystallites are invariably oriented at angles of 0°, 60°, or 120° relative to muscovite (110). Thus, the lepidolite crystallographic plane (*hkl*) which joins muscovite (110) must be located 60° from lepidolite (010) (Fig. 4A). The uninterrupted (001) cleavage plane across both rim and core indicates that the crystallographic direction $\perp$ (001) is parallel in both micas. Accordingly, the lepidolite interplanar angle $(001)\wedge(hkl) = \phi$ must equal the muscovite angle $(001)\wedge(110)$ (Fig. 4B). A value of 85° 05′ was calculated for the muscovite interplanar angle $(001)\wedge(110)$ using refined unit cell parameters from Table 1. Therefore, the lepidolite plane (*hkl*) which joins muscovite must satisfy the two relations $(010)\wedge(hkl) \doteq 60°$ and $(001)\wedge(hkl) \doteq 85°$.

A stereographic projection of lepidolite reveals that no crystallographic plane with small Miller indices exactly satisfies the above conditions. Several planes in the zone $\langle\bar{1}10\rangle$ fulfill the $(010)\wedge(hkl) = 60°$ restriction within one half degree, but indices of $(66\bar{1})$ are required to closely meet the $\phi = 85°$ requirement; for example, the ϕ values of (110), (331), $(44\bar{1})$, $(66\bar{1})$, and $(77\bar{1})$ are 80° 39′, 89° 16′, 87° 05′, 84° 56′, and 84° 19′ respectively. Although $(66\bar{1})$ satisfactorily fulfills the ϕ condition, the possibility exists that a lepidolite plane possessing smaller indices, such as (110), actually joins muscovite and the 4° 26′ misfit in ϕ is accommodated by local lattice distortions. The latter contention is supported by the high degree with which unit cells of muscovite and lepidolite fit along their mutual (110) planes. The percent misfit between mica cells joined along (110) is less than 4.1 percent as calculated from $100(\overline{OL} - \overline{OM})/\overline{OM}$, where $\overline{OL}$ and $\overline{OM}$ are respective lepidolite and muscovite unit cell vectors with common origin at (0,0,0) and terminations at (*a*,*b*,2*c*) and (*a*,*b*,*c*). According to Spry (1969, p. 165) misfits up to 15 percent are frequently encountered between epitaxial overgrowths. Additional data, including single crystal X-ray photographs of joined muscovite-lepidolite crystals, are required to unambiguously determine the indices of the lepidolite plane which joins muscovite (110).

Origin of Lepidolite Rims

Jahns and Burnham (1969) propose that pegmatites develop through crystallization involving both magmatic and supercritical aqueous phases which differ drastically in composition and viscosity. Simultaneous crystallization may occur from both phases, but crystallization from the aqueous phase is believed to continue after complete solidification of the silicate melt. Compositions of both liquid phases, and the compositions of their product crystals, tend to change throughout crystallization. Elements not readily accommodated in the lattices of common rock-forming silicates (*e.g.*, F, Li, Rb, *etc*) are selectively enriched in the aqueous phase; con-

[3] The terms "epitaxy" and "topotaxy" are applied in the strict genetic sense as discussed by Spry (1969, p. 89).

sequently, Li-bearing minerals crystallize primarily from the aqueous phase and the so-called "pockets" develop from the aqueous fluid after the magma is exhausted. Thus, it is apparently possible for an individual pegmatite mineral to crystallize solely from a magma or from an aqueous fluid, but many crystals likely develop through a complex history involving crystallization from both magma and aqueous solutions.

It is difficult to determine with confidence whether the zoned mica crystals grew from a single liquid or were formed by crystallization from two different fluids. As previously noted, the enrichment of Mn and Rb in lepidolite rims may reflect the preferential accommodation of these elements in the 1*M* structure rather than growth from fluids of different composition. On the other hand, closely associated zoned tourmaline, consisting of schorl cores surrounded by alkali tourmaline, seems to support the contention that crystallization from two fluids of different composition occurred. That is, muscovite and schorl crystallized concomitantly from the precursory silicate melt, whereas the rarer pegmatite minerals lepidolite and elbaite formed subsequently from the aqueous fluid.

Prince, Donnay, and Martin (1973) report clear orthoclase overgrowths (on perthite) from "gem pockets" of the nearby Mesa Grande pegmatites; these overgrowths are also enriched in Rb and Cs, again suggesting the presence of late fluids rich in "exotic" elements. Additionally, Munoz (1968, 1971) emphasizes the importance of HF fugacity in the development of lepidolite and was unable to synthesize pure OH end member lepidolite, whereas fluor-lepidolite was readily produced. Presumably F is among the elements concentrated in the late aqueous fluids, again implying that the lepidolite rims formed from a phase chemically distinct from the fluid which produced the muscovite core.

Thus, the zoned tourmaline associated with this zoned mica, in conjunction with results from other investigations, seems to support the contention that two fluids were involved in the crystallization of the zoned crystals; however, Pl enrichment in the outermost muscovite suggests that the transition between fluids may have been gradual. As fluid composition changed, muscovite crystals adjusted their composition, attempting to maintain liquid-solid equilibrium. Ultimately the compositional stability limits of the $2M_1$ structure were exceeded, and subsequent crystallization resulted in the development of expitaxial lepidolite which more readily accommodated Rb and Mn from the fluid phase.

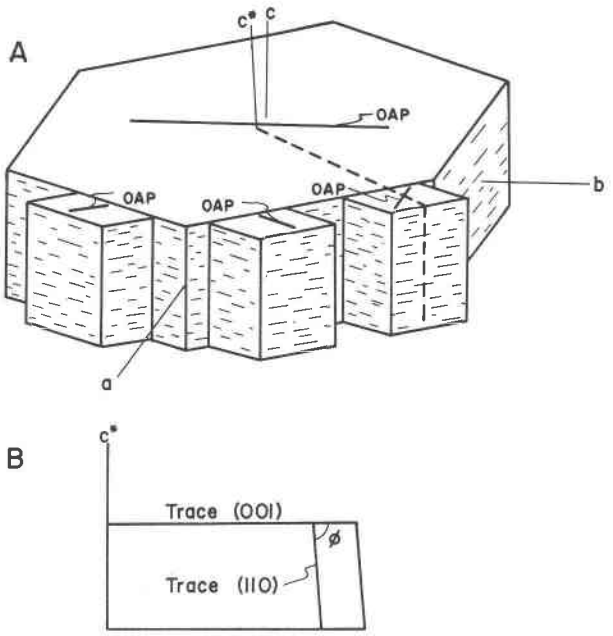

FIG. 4A. Crystallographic relationship between muscovite core and lepidolite crystallites. Lepidolite optic axial planes (parallel to {010}) are indicated by the short bars and invariably give angles of 0, 60, or 120° relative to muscovite (110). Orientations of lepidolite crystallites are related by twinning about ⟨310⟩.

4B. Section perpendicular to muscovite (110) cut along dashed line in Figure 4A. The muscovite angle (001)∧(110) must equal the lepidolite angle $\phi = (001) \wedge (hkl)$ where (hkl) are indices of the lepidolite plane which attaches to muscovite (110).

Acknowledgments

Inland Steel Corporation Research Laboratory kindly provided X-ray diffraction films of mica samples. Chemical analyses were supported by a grant from the Indiana University Foundation.

References

BLOSS, F. D., G. V. GIBBS, AND D. CUMMINGS (1963) Polymorphism and twinning in synthetic fluorophlogopite. *J. Geol.* **71,** 537–547.

BOWMAN, H. L. (1902) On an occurrence of minerals at Haddam Neck, Conn., U.S.A. *Mineral. Mag.* **12,** 97–121.

ČERNY, P., M. RIEDER, AND P. POVONDRA (1970) Three polytypes of lepidolite from Czechoslovakia. *Lithos,* **3,** 319–325.

DEER, W. A., R. A. HOWIE, AND J. ZUSSMAN (1962) *Rock Forming Minerals, Vol. 3, Sheet Silicates.* Longmans, Green and Co., Ltd., London.

FAYE, G. H. (1968) The optical absorption spectra of certain transition metal ions in muscovite, lepidolite, and fuchsite. *Can. J. Earth Sci.* **5,** 31–38.

FOSTER, M. D. (1960) Interpretation of the composition of lithium mica. *U.S. Geol. Surv. Prof. Pap.* **345E.**

GRESENS, R. L., AND H. L. STENSRUD (1971) Chemical, optical, and X-ray analysis of an unusual muscovite-biotite intergrowth. *Lithos,* **4,** 63–69.

HAZEN, R. M., AND D. R. WONES (1972) The effect of cation substitutions on the physical properties of trioctahedral micas. *Am. Mineral.* **57,** 103–129.

HEINRICH, E. W., AND A. A. LEVINSON (1953) Studies of the mica group; mineralogy of the rose muscovites. *Am. Mineral.* **38,** 25–49.

JAHNS, R. H., AND C. W. BURNHAM (1969) Experimental studies of pegmatite genesis. I. A model for the derivation and crystallization of granitic pegmatites. *Econ. Geol.* **64,** 843–864.

———, AND L. A. WRIGHT (1951) Gem- and lithium-bearing pegmatites of the Pala district, San Diego County, California. *Calif. Div. Mines Spec. Rep.* **7A,** 72 p.

MCCAULEY, J. W., AND R. E. NEWNHAM (1971) Origin and prediction of ditrigonal distortions in micas. *Am. Mineral.* **56,** 1626–1638.

MUNOZ, J. L. (1968) Physical properties of synthetic lepidolites. *Am. Mineral.* **53,** 1490–1512.

——— (1971) Hydrothermal stability relations of synthetic lepidolite. *Am. Mineral.* **56,** 2069–2087.

PRINCE, EDWARD, GABRIELLE DONNAY, AND R. F. MARTIN (1973) Neutron diffraction refinement of an ordered orthoclase structure. *Am. Mineral.* **58,** 500–507.

RADOSLOVICH, E. W. (1960) The structure of muscovite. *Acta Crystallogr.* **13,** 919–932.

RIEDER, M. (1970) Chemical composition and physical properties of lithium-iron micas from the Krusne Hory Mountains. *Contrib. Mineral. Petrol.* **27,** 131–158.

SPRY, A. (1969) *Metamorphic Textures.* Pergamon Press, London, 350 p.

TAKEDA, H., N. HAGA, AND R. SADANAGA (1971) Structural investigation of polymorphic transition between $2M_2$, $1M$-lepidolite and $2M$, muscovite. *Mineral. J.* **6,** 203–215.

Manuscript received, January 14, 1974; accepted for publication, June 18, 1974.